

Received 23 March 2023, accepted 27 April 2023, date of publication 18 May 2023, date of current version 31 May 2023.

Digital Object Identifier 10.1109/ACCESS.2023.3277817

RESEARCH ARTICLE

A Novel Cross-Layer Adaptive Fuzzy-Based Ad Hoc On-Demand Distance Vector Routing Protocol for MANETs

FATEMEH SAFARI¹, HERB KUNZE², JASON ERNST¹, AND DANIEL GILLIS¹

¹School of Computer Science, University of Guelph, Guelph, ON N1G 1Y4, Canada

²Department of Mathematics and Statistics, University of Guelph, Guelph, ON N1G 2W1, Canada

Corresponding author: Fatemeh Safari (safari@uoguelph.ca)

This work was supported in part by Mitacs, in part by the Natural Sciences and Engineering Research Council of Canada, and in part by the University of Guelph.

ABSTRACT One of the essential processes in Mobile Ad hoc Networks (MANETs) is blind flooding to discover routes between source and destination mobile nodes. As the density of nodes in the network increases, the number of broadcast packets increases exponentially. This can lead to broadcast storms, a drain on the device's battery, and reduced network efficiency. We propose a Cross-layer Adaptive Fuzzy-based Ad hoc On-Demand Distance Vector routing protocol (CLAF-AODV) to minimize the routing broadcast traffic by considering the quality of service (QoS) (e.g. delay, throughput, packet loss), stability, and adaptability of the network. The suggested method employs two-level fuzzy logic and a cross-layer design approach to select the appropriate nodes with a higher probability of participating in broadcasting by considering parameters from the three first layers of the Open Systems Interconnection (OSI) model to achieve a quality of service, stability, and adaptability. It not only investigates the quality of the node and the network density around the node to make a decision but also investigates the path that the broadcast packet traveled to reach this node. Simulation results reveal that our proposed protocol reduces the number of broadcast packets and significantly improves network performance with respect to throughput, packet loss, normalized routing load, collision rate, and average energy consumption compared to the standard AODV and the Fixed Probability AODV (FP-AODV) algorithms.

INDEX TERMS Broadcast storm, broadcasting, fuzzy logic, mobile ad hoc network, quality of service, route discovery, routing protocol.

I. INTRODUCTION

Mobile Ad hoc Networks (MANETs) have been shown to be important to current and future communication methods, facilitated in part by advancements in wireless technologies and the ubiquity of mobile devices [1]. Although there are many potential applications for MANETs (see [2] for examples), there are still several substantial challenges and unresolved problems [3] - the most significant and challenging being that of routing [4]. In this study, we focus on routing challenges in high-density Mobile Ad hoc Networks.

The associate editor coordinating the review of this manuscript and approving it for publication was Nafees Mansoor¹.

Almost every MANET routing protocol relies on a broadcast scheme to distribute routing information through the network [5]. The fundamental mechanisms in route discovery in reactive routing protocols are based on broadcasting techniques through nodes from sources to destinations to find existing paths [6]. Nodes in MANETs are mobile and their mobility leads to frequent route failures and the need for ongoing route discovery [7]. While broadcasting increases the reachability of the route request messages to the destinations in sparse networks, rebroadcasting causes an excessive number of redundant packets across the high-density networks that significantly decrease network performance [8]. Due to resource constraints (e.g. media access, limited bandwidth, and battery power), this redundant traffic

is undesired because it reduces network performance [8]. Therefore, the routing discovery process involves producing overhead that cannot be overlooked.

A key challenge in the development of MANET routing algorithms is to create more effective broadcast techniques that can adjust to topology changes quickly while also taking into account channel conditions, link bandwidth, congestion, and battery power of mobile devices.

This study's main goal is to investigate improvements to network performance by suppressing broadcast routing load in the phase of route discovery. We propose a Cross-layer Adaptive Fuzzy-based Ad hoc On-demand Distance Vector routing protocol (CLAF-AODV) to reduce routing broadcast traffic by considering the factors that affect the quality of service (i.e. bandwidth, queue length), stability (i.e. node energy, received signal strength), and adaptability with the network density. We follow a hybrid approach to broadcast decision-making by considering three phases and employing fuzzy logic and cross-layer design. The suggested adaptive hybrid rebroadcasting protocol prevents broadcast storms in highly dense networks while maintaining reachability in a sparse network. The resulting CLAF-AODV protocol is then compared against standard AODV and FP-AODV protocols.

This article is structured as follows: An overview of the existing routing protocols is given in Section II. Section III outlines the proposed algorithm, which is then evaluated via a simulation study in Section IV. Results and discussions are provided in Sections V and VI. Finally, we conclude our work in Section VII.

II. EXISTING PROTOCOLS

Various rebroadcasting approaches have been used to reduce or avoid redundant packet forwarding with the aim of developing optimal routing solutions [9]. The difference between these techniques is in the decision-making policies and parameters used for forwarding broadcast packets.

A. BROADCASTING MECHANISMS

Flooding is the basic mechanism for sending a packet from a source to a particular target node. In *simple flooding* (also known as *blind flooding*), the source node broadcasts a data packet to all its neighbours. The neighbours repeat this procedure until the packet reaches its destination. The Ad hoc On-demand Distance Vector (AODV) is an example of a simple flooding routing protocol [10]. The serious disadvantage of flooding is that it produces excessive redundant traffic (i.e. *broadcast storms*), which wastes network resources (e.g. bandwidth, battery), especially in high-density network environments. These issues can impair network functionality and lead to packet loss, end-to-end delay, increased latency, and low throughput [11].

A *deterministic strategy* that lets a selected number of nodes take part in broadcasting by building a *virtual overlay network* is one way to overcome this problem [12]. Global topological information is required to select the subset of nodes. *Connected dominating set (CDS)* [13] and

Multi-point relay (MPR) [14] are two common strategies for this broadcasting approach. The CDS technique selects a subset of the network's nodes as the connected backbone (also known as the virtual backbone), such that every other node in the network has at least one neighbour in the subset. Finding a minimum CDS in a given network is a challenging task [15]. In the case of MPR, every node in the MANET chooses a subset of its one-hop neighbour nodes that are responsible for rebroadcasting any received broadcast packets (called a multi-point relay). In this scenario, neighbour nodes that are not in the MPR set receive the broadcast packets and discard them.

Most deterministic broadcasting algorithms rely on the network topology and its backbone. In low-mobility network environments, issues have been raised about the repeated use of the same nodes that can result in unbalanced energy consumption, unbalanced load, etc. This class of algorithm involves the periodic exchange of topological information to maintain or select the MPR or CDS sets. In high-mobility network conditions (where the network topology can change rapidly), a high number of control messages should be sent to maintain up-to-date topological information. However, this may result in a large number of collisions as well as a high rate of packet loss [16]. Depending on the application, offering a virtual structure over a real network topology may or may not be advantageous enough to justify the expense of building and maintaining it.

Counter-based techniques attempt to resolve the problem by preventing a mobile node from rebroadcasting a message if the number of duplicate broadcast packets received by the node during a random wait period exceeds a threshold value [17]. *Fixed-counter* strategies are incapable of performing well in different network operating conditions. A low counter threshold saves a lot of re-transmission, but reachability suffers greatly in sparse networks. A large value for this threshold, on the other hand, indicates strong reachability but poor savings on broadcast packets. To address this, some researchers have proposed *dynamic thresholds* to improve broadcasting efficiency. For example, [18] uses three dynamic thresholds to consider network distribution as dense, medium, or sparse. The network density is determined by counting HELLO packets received from neighbours. The mobile nodes rebroadcast the message while taking the node density into consideration if the number of duplicate broadcast packets received falls below a certain threshold [18]. Authors in [19] present an adjustable counter-based algorithm by using network density as a parameter to define Random Assessment Delay (RAD) (random wait timer). For dense networks, a small RAD is employed, and for sparse networks, a big RAD is. These schemes were found to improve throughput and reachability but at the expense of longer delays.

Probabilistic techniques cut down on the number of broadcasting nodes by assigning a forward probability P to the nodes (that is, nodes do not participate in broadcasting, with a probability of $1 - P$). The challenging part of these techniques is choosing P . Numerous authors have explored the

use of both fixed and dynamic probabilistic broadcasting approaches [20]. Unique fixed probability is not effective for different network densities (small values of P are effective for high-density networks, while high values of P are needed if the network is sparse [21]). To overcome the limitation of fixed probability, several dynamic probabilistic approaches have been proposed. A probabilistic extension to the AODV protocol [22] used a threshold-based probabilistic method for making decisions about the route request forwarding probability. Specifically, the protocol first calculates a threshold value for the average number of neighbour nodes, then given the total number of network nodes, determines if the localized network around each node is sparse or dense. If a node's localized network has fewer neighbours than a threshold, it is labeled sparse. In this case, the node forwards the RREQ with a probability of $P1$. The localized network is designated dense when a node's number of neighbours surpasses the threshold, and the broadcast probability is set to $P2$, where $P1 > P2$. Unfortunately, it is not always possible in real-world applications for the algorithm to know how many nodes are present in the network as a whole. Furthermore, there are no criteria for selecting high-quality nodes to participate in routing. Other methods, such as the Gossip-based node residual energy AODV approach [23], computes dynamic rebroadcasting probabilities based on residual energy, node received signal power, and node density to reduce network overhead. When an RREQ is received, the received signal strength is compared to a threshold. If it falls below the threshold, then the RREQ is discarded. Otherwise, the normalized minimum residual energy from the source to the current node is used to compute the forwarding probability P . If a node drops the RREQ packet, it checks if the packet has or has not been received by its neighbour to prevent an early death of the routing packet. In this case, the node sets a *gossiping* timer C based on the network density, then waits to hear if a copy of the RREQ has been received. If it does not receive an RREQ during the gossip period, it re-transmits the RREQ. While the protocol is energy aware, it does not consider quality metrics to calculate the routing probability. Alternatively, the topology-aware Fuzzy controlled probabilistic broadcast method [24] uses hop count and downlink neighbour coverage to determine a node's probability of rebroadcasting. Reference [25] introduced a dynamic fuzzy energy state-based AODV (DFES-AODV) that calculated the RREQ forwarding probability using a Mamdani fuzzy logic system (see [26] for details on Mamdani Fuzzy logic). The inputs for the DFES-AODV algorithm include the residual battery level of a node as well as its energy drain rate. It is advantageous to choose the probability of broadcasting in a way that takes into account QoS requirements in addition to network density.

Several dynamic probabilistic approaches have also been proposed in which a variety of criteria are used to determine the forward probability. For example, [27] proposed a two-phase probabilistic algorithm that used a second-timed

broadcasting scheme based on signal-strength and GPS-derived distances to calculate forward probability and random assessment delay (see [8] for more details). Node mobility and link stability have also been considered in [28] to propose a probabilistic broadcasting algorithm to predict stable links that are involved in routing paths. Choosing the node's/network's parameters and figuring out how to use them to generate an adaptive probability is the biggest challenge in dynamic probabilistic techniques.

In *area-based* algorithms, the network coverage area of each node is used to inform rebroadcasting decisions. Specifically, a receiver node rebroadcasts received packets if doing so will increase the coverage area. In the case of the Based Beacon-less Algorithms proposed in [29], each node starts a timer as soon as it receives a message's first copy. The node continues to receive more copies of the exact same message so long as the timer has not expired. If node A (for example) receives a message from several sources and these sources cover the transmission range of A , node A discards the received broadcast message. The AOMDV-DREAM protocol [30] combines the ad hoc on-demand multipath distance vector (AOMDV) protocol with the Distance Routing Effect Algorithm for Mobility (DREAM) protocol. With the help of this technique, the number of broadcast messages in the network can be reduced by estimating the target location. The area-based technique struggles with node mobility since nodes constantly need to update their position data, adding to the overhead [31]. In addition, the use of GPS and position information is required for area-based approaches, which places limitations on some applications.

Neighbour-knowledge methods use neighbour information to decide whether or not to rebroadcast a message or not. Although nodes have a greater awareness of their neighbourhood thanks to neighbour-knowledge techniques, it might be challenging to have reliable and up-to-date information in highly mobile networks. The authors in [32] defined a *self-pruning technique* that reduces the number of redundant broadcast messages based on three-hop neighbour knowledge. In self-pruning techniques, a sender node adds information about its neighbour in the packet header and the receiver node compares this information with its table to decide about rebroadcasting. The Scalable Broadcast Algorithm [33] is similar to self-pruning but uses *Hello messages* to propagate 2-hop neighbour knowledge. Extended Neighbourhood Knowledge based Dominant Pruning is proposed in [34] and uses a *dominant pruning technique* to decrease the number of unnecessary broadcast packets by using 3-hop Neighbour connectivity information. In dominant pruning, source nodes choose some of their neighbours that are allowed to rebroadcast. The addresses of selected nodes are added to the broadcast message header and nodes that find their address in the received message are permitted to rebroadcast. Neighbour knowledge-based methods decided whether to broadcast based on information received from neighbour nodes. The

neighbour information overhead increases with an increase in network density or size [35].

Finally, *hybrid broadcast* schemes optimize MANET broadcasting by combining the benefits of two or more methods to achieve better routing performance. An adaptive probabilistic broadcasting technique was proposed in [27] based on Neighbour knowledge and a forwarding zone criterion. The algorithm considers the density of nodes using a density metric called expansion metric. Reference [36] combined the benefits of probabilistic and counter-based schemes to suggest an efficient counter-based scheme (ECS). When a node receives a fresh broadcast packet in ECS, it begins a timer and keeps track of how many additional identical broadcast packets it receives. The packet is dropped if this value is greater than a preset threshold; otherwise, it is replayed with a probability of P . Dynamic Connectivity Factor Routing Protocol [37] decreases the RREQ overhead by using a *connectivity metric* (i.e. density information) and *dynamic connectivity factors* (i.e. a node's connectivity ratio based on its neighbourhood information), to compute the forwarding probability. The Neighbour Knowledge-based Rebroadcast protocol, which combines Neighbour coverage knowledge and probabilistic approaches, was proposed by the authors in [38] to achieve good QoS. The Global Positioning System (GPS) or signal strength can be utilised to calculate the distance between the source and destination nodes in this scenario, which determines the rebroadcast probability.

It is concerning that some research articles fail to include key details about the simulation setting, making it more difficult to accurately reproduce the study [39].

B. AODV ROUTE DISCOVERY PROCEDURE

One of the most popular reactive routing protocols that has been extensively employed in the field of mobile wireless research is the AODV protocol. Unlike proactive routing protocols, an AODV node does not keep any routing information about all of the network's potential destinations. Routes are found on-demand by starting a route discovery process based on simple flooding (blind flooding). In simple flooding, when a mobile node has data for a specific destination, it broadcasts a route request (RREQ) packet towards its neighbours in search of a particular destination. Any nodes that receive the RREQ rebroadcast it until it reaches its destination. After receiving the RREQ, the destination sends a route reply (RREP) in the opposite direction to the source node (Refer to [40] for more detailed information about AODV operation). Blind flooding of RREQ messages at the phase of route discovery can cause a significant number of duplicated packets (RREQs) which utilize the network resources inefficiently and have negative effects on end-to-end delay, packet loss, throughput, etc.

III. A CROSS-LAYER HYBRID ROUTE DISCOVERY ALGORITHM WITH FUZZY LOGIC

This section explains the suggested route discovery mechanism for reactive routing protocols in MANETs that adjusts to

the network changes including the quality of nodes (in terms of queue length, channel congestion, and remaining energy), quality of the links (in terms of bandwidth and received signal strength), and the network density surrounding the nodes. The suggested method takes advantage of three techniques to provide a good trade-off between minimal communication overhead and quality of service: 1) threshold-based retransmission, 2) probabilistic retransmission and, 3) counter-based mechanism to control routing overhead. Threshold-based transmission considers the minimum requirements of a node for participating in the routing process. In addition, if the network density is below the predefined threshold, the node certainly transmits the received broadcast packets. We use fuzzy logic to calculate broadcast probability for the receiver nodes based on node quality, network density as well as the path quality that the broadcast packet traverse on it. Finally, to avoid the unreachability of broadcast packets, we use the counter-based algorithm to ensure an adequate number of nodes in the network propagate the broadcast packets. The proposed hybrid rebroadcasting technique is applied to an AODV protocol which is one of the most popular reactive routing protocols for MANETs.

MANET is a distributed system that has neither central management nor central monitoring system. Therefore, mobile nodes are unable to have a full view of the network condition to make decisions about their operation. In addition, gathering global information is not practical because of restricted resources in MANET such as bandwidth or node hardware.

In this study, a *cross-layer* design is employed to help mobile nodes learn about network conditions by analyzing local parameters at different OSI layers. The route discovery algorithm uses information from the physical layer and data link layer as shown in Fig. 1. Routing protocols operate in layer three. Although higher-layer protocols do not directly interact with the physical layer, the physical layer and data link layer characteristics in wireless communication have an impact on the performance of higher-layer protocols. Therefore, these layers should not be ignored for high-performance routing protocols. We're looking for characteristics in several layers that affect adaptability, stability, and quality which have been discussed later in this section. To the best of our knowledge, none of the previous studies take into account adequate factors to make the best decision regarding choosing the best nodes for rebroadcasting.

To deal with broadcast storms in high-density MANETs, a fuzzy logic solution with the consideration of cross-layer parameters as the inputs is suggested to make appropriate decisions about RREQ forwarding. Fuzzy logic, proposed by Zadeh [41], is employed in many applications that require control or decision-making because it delivers low-cost answers. Fuzzy logic is a soft computing technique that can produce precise and accurate decisions in situations that are multi-variable, uncertain, and imprecise. Fuzzy logic takes advantage of uncertainty to produce approximate decisions that can be employed in MANET routing. The other

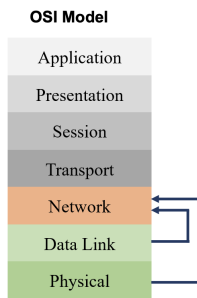


FIGURE 1. Cross-layer design between physical, data link, and network layers within the Open Systems Interconnection (OSI) model.

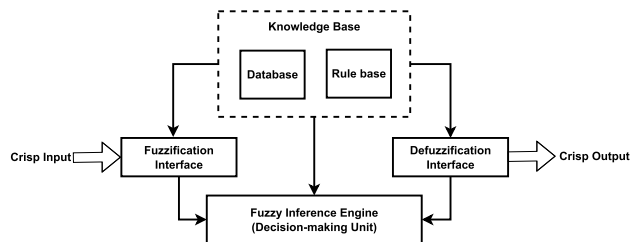


FIGURE 2. The proposed Fuzzy Inference System is comprised of four main blocks: the Fuzzification Interface, the Fuzzy Inference Engine (Decision-making unit), the Defuzzification Interface, and the Knowledge Base.

benefits of adopting the fuzzy logic system are its simplicity and low computational requirements [42].

The proposed algorithm is implemented with *Mamdani* fuzzy inference system. The *Mamdani* type model is a fuzzy relational model in which each linguistic control rule is represented by an IF-THEN statement to define the antecedents and consequent. Each rule produces a fuzzy set as its output (Fig. 2). The proposed algorithm contains the monitoring and fuzzy analyzing module, and the broadcast decision-maker module.

The objective of the proposed fuzzy model is to identify the most appropriate nodes by considering network density, node quality and stability factors to participate in the route discovery process with the aim of creating a high-quality path between a source and destination node. The most appropriate nodes are not only selected based on the local properties of the nodes, but also we define a new parameter that indicates the quality of the path that RREQ packet travels on it to this node. These nodes participate in routing with higher probability.

A. MONITORING AND FUZZY ANALYZING MODULE

A cross-layer fuzzy monitoring system is implemented in each mobile node to calculate the Node Quality Metric (*NQM*) (see Fig. 3). The embedded monitoring system monitors the Received Signal Strength (RSS) at the physical layer, the remaining energy of the node, the average size of the contention window, the average queue length and available bandwidth at the medium access control (MAC) layer, and the number of neighbours from the network layer when receiving

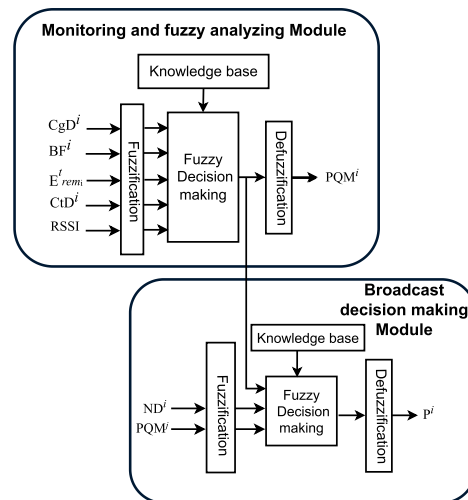


FIGURE 3. An overview of the fuzzy subsystems of the cross-layer hybrid route discovery system with fuzzy logic outlined in Fig. 2.

each RREQ message. The quality of the node is determined based on a fuzzy inference system (FIS).

1) FUZZY INPUTS

There are five input parameters for the fuzzy logic decision-maker block including Queue congestion Degree (*CgD*), Bandwidth Factor (*BF*), Remaining Energy (*E_{rem}*), Contention Degree (*CtD*), and Received Signal Strength Indicator (*RSSI*). These parameters are used by the decision-maker to estimate network quality and stability (see Table 1 for the fuzzy rules used by this module). Each is described below.

a: QUEUE CONGESTION DEGREE (*CgD*)

During the network routing process, routers use buffers as memory blocks to handle data transmission. The router or mobile node places packets in a buffer (also known as a queue) until it transmits them on wireless media. The queue length can describe the amount of traffic that is handled by the mobile node. The size of the queue is limited. If the rate of input traffic exceeds the rate of output traffic, the queue capacity becomes full and congestion occurs. In the case of congestion, packets are dropped based on a predefined policy. Dropping the packets degrades network performance and *quality of service*. Therefore the size of queue occupancy can be used as a factor of quality. The average queue occupancy [43] of a mobile node at time *t* can be calculated using the Exponentially Weighted Moving Average formula in Eq. (1):

$$Q_{avg(t)}^i = \alpha Q_{cur}^i + (1 - \alpha) Q_{avg(t-1)}^i, \tag{1}$$

where the weight factor $\alpha \in (0, 1)$, Q_{cur}^i is the current queue size of node *i*, and $Q_{avg(t-1)}^i$ is average queue occupancy of node *i* at time *t* - 1.

The queue congestion degree CgD^i of node i can be measured in packet buffer occupancy rate using Eq. (2):

$$CgD^i = Q_{avg(t)}^i / Q_{size}, \quad (2)$$

where $Q_{avg(t)}^i$ is the average queue length for node i at the time t and Q_{size} is the node i queue (buffer) capacity.

b: BANDWIDTH FACTOR (BF)

Bandwidth is a determining factor in *service quality* which can be measured at the physical layer. If the available bandwidth is insufficient, queuing delays increase and congestion may occur. Congestion occurs when a node or link carries more data than it is capable of handling. If some packets are discarded due to congestion (packet loss), they must be retransmitted, resulting in further delay. The bandwidth factor indicates the percentage of available bandwidth. IEEE 802.11 DCF wireless channel is *busy* when the mobile node receives or transmits data packets; otherwise, it is *idle*. The Eq. (3) is used to calculate the bandwidth factor for node i :

$$BF^i = T_{Idle}(t) / T_{int}, \quad (3)$$

where T_{Idle} represents the accumulative idle time periods T_{idle} in the predefined time period T_{int} (2 seconds in this work [44]) which is given in Eq. (4):

$$T_{Idle}(t) = \sum_t^{t+T_{int}} T_{idle} \quad (4)$$

c: REMAINING ENERGY (E_{rem})

MANET network nodes rely heavily on their limited battery energy. The available energy level of nodes is an important factor for *path stability*. If the path contains even one low-energy node, there is a high chance of link failure during packet transmission. The rate of energy utilization is defined in Eq. (5):

$$EU_i = (P_r \times N_r + P_s \times N_s) \quad (5)$$

where energy utilization by the node i when it is receiving or sending a packet are P_r and P_s respectively; N_r and N_s are the number of received and sent packets in turn, where P_r and P_s are the energy utilized by the node i when it is receiving or sending a packet; N_r and N_s are the number of the two types of packets. The percentage of remaining energy for node i is defined in Eq. (6):

$$E_{rem_i}^t = (E_{max_i} - EU_i^t) / E_{max_i}, \quad (6)$$

where E_{max_i} is the initial energy of node i .

d: CONTENTION DEGREE (CtD)

Back-off is a technique to improve channel access and reduce collision probabilities in the Distributed Coordination Function of IEEE 802.11 medium access control (MAC) model when multiple nodes want to send data simultaneously. If a

node encounters a collision, it waits for a back-off time called the contention window (CW) for subsequent data transmission. The contention window is $[CW_{min}, CW_{max}]$ where CW_{min} and CW_{max} are the minimum and maximum contention window sizes, respectively. Collision in the channel causes an exponential increase in CW until it reaches its maximum value. The contention window moves to the minimum (CW_{min}) if data is successfully transmitted or if it reaches the maximum value as a result of the exponential increase due to collision. More mobile nodes in the vicinity of a node cause contention and a bigger contention window size. Lower contention window size indicates less collision and provides *higher quality* and better performance in terms of end-to-end delay and packet drop. The average contention window for a mobile node can be calculated using the Exponentially Weighted Moving Average (EWMA) formula in Eq. (7):

$$CW_{avg(t)}^i = \alpha CW_{cur} + (1 - \alpha) CW_{avg(t-1)}^i, \quad (7)$$

where $\alpha \in (0, 1)$, CW_{cur} is the current CW size of node i and $CW_{avg(t)}^i$ is average CW of node i at time t . We captured the value of the contention window every 2 seconds. We captured the value of the contention window every 2 seconds.

The contention degree CtD for node i is determined via Eq. (8):

$$CtD^i = CW_{avg(t)}^i / CW_{max} \quad (8)$$

e: RECEIVED SIGNAL STRENGTH INDICATOR (RSSI)

In wireless networks, the power of a signal typically decreases proportionally with the square of the distance (referred to as path loss), and as a result of other factors (e.g. physical obstructions, wireless frequency interference, signal reflection, noise level). To keep things simple, we assume that distance is the only parameter that affects signal strength. The relation between the received signal and distance is shown in Eq. (9):

$$\text{Received signal power} \propto \frac{1}{d^2} \quad (9)$$

where d is the distance between two nodes.

The received signal strength indicates *link stability*. Lower RSSI represents longer distances between the receiver and sender nodes, which could result in a higher probability of link failure. In addition, higher signal strength provides higher bandwidth.

2) FUZZY OUTPUTS

As shown in Fig. 3, the output of this module, (NQM), is used for two purposes. First, the crisp NQM value is used to calculate the path quality metric (PQM). Second, the fuzzy value of NQM is used as an input parameter for the second-level fuzzy system to calculate the RREQ retransmission probability.

We modified the RREQ message by adding the PQM field in the original messages (Fig. 4). The path quality metric for node i (PQM_i) indicates path quality that RREQ traverses to

TABLE 1. Fuzzy rules used for monitoring and analyzing module. Input 5-tuples outline high (H), medium (M), and low (L) classifications for remaining energy, bandwidth, congestion, contention, and RSS, respectively. Output labels include very low (VL), medium (M), and high (H).

Rule	Input	Output	Rule	Input	Output	Rule	Input	Output
1	(L, L, L, L, H)	L	37	(L, L, L, L, L)	L	73	(L, L, L, L, M)	L
2	(L, L, L, M, H)	L	38	(L, L, L, M, L)	L	74	(L, L, L, M, M)	L
3	(L, L, L, H, H)	L	39	(L, L, L, H, L)	L	75	(L, L, L, H, M)	L
4	(L, L, M, L, H)	L	40	(L, L, M, L, L)	L	76	(L, L, M, L, M)	L
5	(L, L, M, M, H)	L	41	(L, L, M, M, L)	L	77	(L, L, M, M, M)	L
6	(L, L, M, H, H)	L	42	(L, L, M, H, L)	L	78	(L, L, M, H, M)	L
7	(L, L, H, L, H)	L	43	(L, L, H, L, L)	L	79	(L, L, H, L, M)	L
8	(L, L, H, M, H)	L	44	(L, L, H, M, L)	L	80	(L, L, H, M, M)	L
9	(L, L, H, H, H)	L	45	(L, L, H, H, L)	L	81	(L, L, H, H, M)	L
10	(L, H, L, L, H)	M	46	(L, H, L, L, L)	M	82	(L, H, L, L, M)	M
11	(L, H, L, M, H)	M	47	(L, H, L, M, L)	M	83	(L, H, L, M, M)	M
12	(L, H, L, H, H)	L	48	(L, H, L, H, L)	L	84	(L, H, L, H, M)	L
13	(L, H, M, L, H)	M	49	(L, H, M, L, L)	M	85	(L, H, M, L, M)	M
14	(L, H, M, M, H)	M	50	(L, H, M, M, L)	M	86	(L, H, M, M, M)	M
15	(L, H, M, H, H)	L	51	(L, H, M, H, L)	L	87	(L, H, M, H, M)	L
16	(L, H, H, L, H)	L	52	(L, H, H, L, L)	L	88	(L, H, H, L, M)	L
17	(L, H, H, M, H)	L	53	(L, H, H, M, L)	L	89	(L, H, H, M, M)	L
18	(L, H, H, H, H)	L	54	(L, H, H, H, L)	L	90	(L, H, H, H, M)	L
19	(H, L, L, L, H)	L	55	(H, L, L, L, L)	L	91	(H, L, L, L, M)	L
20	(H, L, L, M, H)	L	56	(H, L, L, M, L)	L	92	(H, L, L, M, M)	L
21	(H, L, L, H, H)	L	57	(H, L, L, H, L)	L	93	(H, L, L, H, M)	L
22	(H, L, M, L, H)	L	58	(H, L, M, L, L)	L	94	(H, L, M, L, M)	L
23	(H, L, M, M, H)	L	59	(H, L, M, M, L)	L	95	(H, L, M, M, M)	L
24	(H, L, M, H, H)	L	60	(H, L, M, H, L)	L	96	(H, L, M, H, M)	L
25	(H, L, H, L, H)	L	61	(H, L, H, L, L)	L	97	(H, L, H, L, M)	L
26	(H, L, H, M, H)	L	62	(H, L, H, M, L)	L	98	(H, L, H, M, M)	L
27	(H, L, H, H, H)	L	63	(H, L, H, H, L)	L	99	(H, L, H, H, M)	L
28	(H, H, L, L, H)	H	64	(H, H, L, L, L)	M	100	(H, H, L, L, M)	H
29	(H, H, L, M, H)	M	65	(H, H, L, M, L)	M	101	(H, H, L, M, M)	M
30	(H, H, L, H, H)	L	66	(H, H, L, H, L)	L	102	(H, H, L, H, M)	L
31	(H, H, M, L, H)	M	67	(H, H, M, L, L)	M	103	(H, H, M, L, M)	M
32	(H, H, M, M, H)	M	68	(H, H, M, M, L)	M	104	(H, H, M, M, M)	M
33	(H, H, M, H, H)	L	69	(H, H, M, H, L)	L	105	(H, H, M, H, M)	L
34	(H, H, H, L, H)	L	70	(H, H, H, L, L)	L	106	(H, H, H, L, M)	L
35	(H, H, H, M, H)	L	71	(H, H, H, M, L)	L	107	(H, H, H, M, M)	L
36	(H, H, H, H, H)	L	72	(H, H, H, H, L)	L	108	(H, H, H, H, M)	L

Original RREQ packet

Type	Flags	Reserved	Hop Counts
RREQ (Broadcast) ID			
Destination IP address			
Destination sequence number			
Original IP address			
Originator sequence number			

Modified RREQ packet

Type	Flags	Path Quality Metric	Hop Counts
RREQ (Broadcast) ID			
Destination IP address			
Destination sequence number			
Original IP address			
Originator sequence number			

FIGURE 4. An overview of the original RREQ packet (as described in [40]), and the modified RREQ packet which replaces the reserved message with the Path Quality Metric.

node i , and is determined via Eq. (10):

$$PQM_i = \frac{1}{n+1} (n \times PQM_j + NQM_i), \quad (10)$$

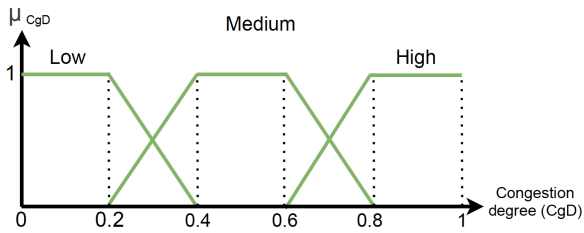
where PQM_j is the embedded path quality metric in RREQ received from node j , and n is the hop count. Node i modifies the received RREQ with this value before its transmission.

3) KNOWLEDGE BASE BLOCK

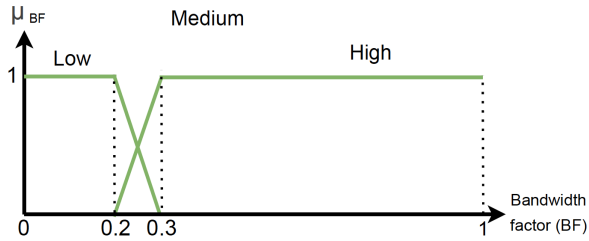
The system’s intelligence is stored in the knowledge base block which contains two inner blocks: 1) the database block in which the membership functions of fuzzy sets are defined, and 2) the rule-based block which includes fuzzy IF-THEN rules.

Three fuzzy sets with trapezoidal membership functions were created for the congestion degree (CgD), contention degree (CtD), and received signal strength (RSS) variables. The three input linguistic variables were utilized to assign three levels to these input parameters: low (L), medium (M), and high (H). Furthermore, the trapezoidal membership function is defined by two linguistic expressions: low (L), and high (H) to describe fuzzy sets for available bandwidth and remaining energy (Fig. 5(a-e)). To define the linguistic values for contention degree we consider its crisp value given a certain number of attempts (Table 2). Finally, we use the values of signal strength given a particular distance between two mobile nodes to determine the linguistic values for signal strength (Table 3).

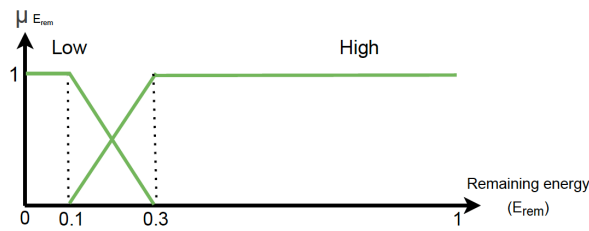
The parameter *Node Quality Metric (NQM)* is considered as the output for the monitoring and analyzing module. It has been described with three fuzzy sets (linguistic variables) with trapezoidal membership functions: low, medium, and



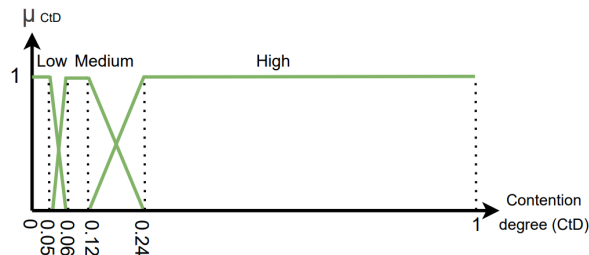
(a) Membership function of the congestion degree input.



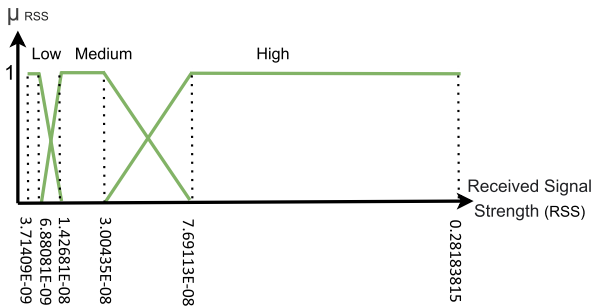
(b) Membership function of the bandwidth factor input.



(c) Membership function of the remaining energy input.



(d) Membership function of the contention degree input.



(e) Membership function of the Received Signal Strength Indicator input.

FIGURE 5. Fuzzy membership sets of the input variables for the monitoring and analyzing module.

high. The output membership function for NQM is shown in Fig. 6.

TABLE 2. The value of contention window (CW) and contention degree (CD) according to the attempt number.

Attempt #	N	CW(2 ^N - 1)	Contention Degree
1	5	31	0.00097752
2	6	63	0.06158358
3	7	127	0.12414467
4	8	255	0.24926686
5	9	511	0.49951124
6	10	1023	1.00000000

TABLE 3. The value of signal strength according to the distance (m) between two mobile nodes.

Distance (m)	Signal Strength
0	2.81838E-01
50	7.69113E-08
80	3.00435E-08
100	1.42681E-08
120	6.8881E-09
150	3.7149E-09

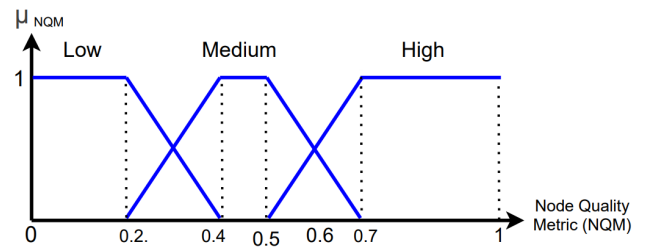


FIGURE 6. Fuzzy membership sets of the output variable (NQM) for the monitoring and analyzing module.

Fuzzy rules are IF-THEN rules designed to make decisions on the quality of the mobile node. As demonstrated earlier, CgD, CtD and RSS parameters described with three linguistic variables and two linguistic variables have been employed for available bandwidth and remaining energy. It results in $3 \times 3 \times 3 \times 2 \times 2 = 108$ rules (Table 1). There are two parts for each fuzzy rule. The first part is the introduction (IF) and the second part is the result (THEN). For example, IF remaining energy is high AND available bandwidth is high AND congestion degree is medium AND contention degree is low AND signal strength is high, THEN node quality is medium (see rule 31, Table 1). The trapezoidal membership functions are used by the fuzzification block to generate an appropriate fuzzy result for all crisp input parameters as shown in Fig. 5(a-e).

The fuzzy output of the analysis and monitoring module (i.e. NQM) is used as the input of the Broadcast decision-maker module. Additionally, PQM, which must be included in the RREQ packet, is calculated using this output. As such, the defuzzification block produces the equivalent crisp value for NQM (fuzzy output). To provide crisp output for NQM, we employ the Last of Maxima (LOM) as a defuzzification method.

B. BROADCAST DECISION-MAKER MODULE

The mobile node makes a decision regarding transmitting or dropping the received RREQ message using the broadcast

decision-maker module. Fig. 7 shows the process of RREQ forwarding. A source node broadcasts an RREQ packet once it desires to send data to a destination node. When an intermediate node n receives the RREQ packet, it checks three conditions. The first condition is to determine if the packet is received on a bidirectional link. Then it checks whether the packet is not a duplicated RREQ that was forwarded before. Finally, the protocol searches its routing table for the requested destination. If it finds the destination address in its routing table, it sends an RREP message toward the source node and discards the received RREQ (which follows that AODV proposal). However, if this is not the case, the proposed algorithm executes the three phases of its decision-making process.

Phase I: First, a node measures the RSS of the sender, and its own remaining power to verify the minimum requirement for participating in the routing process to avoid route failure in the very near future. If it does not meet the minimum requirement, it drops the RREQ; otherwise, it goes to the next step. The number of neighbours for node i is defined as node degree ND . If the node degree of node n is less than the minimum value of ND_{thr} then it means the network is sparse and all nodes should participate in route discovery. Therefore node n rebroadcasts the RREQ with probability 1. If the node degree is greater than the threshold, the node makes a decision about the forwarding probability based on network density, quality factors, and stability factors.

Phase II: At this step, the node utilizes fuzzy logic control to make an appropriate decision. The inputs of the fuzzy block are cross-layer parameters that help to make a precise forwarding decision. As illustrated in Fig. 3, there are three inputs for this module: node degree ND , node quality metric NQM , and path quality metric PQM . The output of this fuzzy system is an appropriate forwarding probability P for the RREQ. Before we describe Phase III, we provide a summary of the fuzzy inputs for the broadcast decision-maker.

1) FUZZY INPUTS

a: NODE DEGREE (ND)

The number of neighbours, which also is referred to as node degree, can be an indication of network density around the mobile node. While all nodes should participate in broadcasting in sparse networks to guarantee reachability, in a dense network, the probability of rebroadcasting should be a factor of node density. This parameter can be calculated as the length of the neighbour table or routing table.

b: NODE QUALITY METRIC (NQM)

The fuzzy output of the *monitoring and fuzzy analyzing module* (Fig. 3) is used as one of the inputs for the second fuzzy subsystem to calculate the RREQ forwarding probability. This factor reflects the quality of nodes, wireless channel and stability of the link that the RREQ received on it.

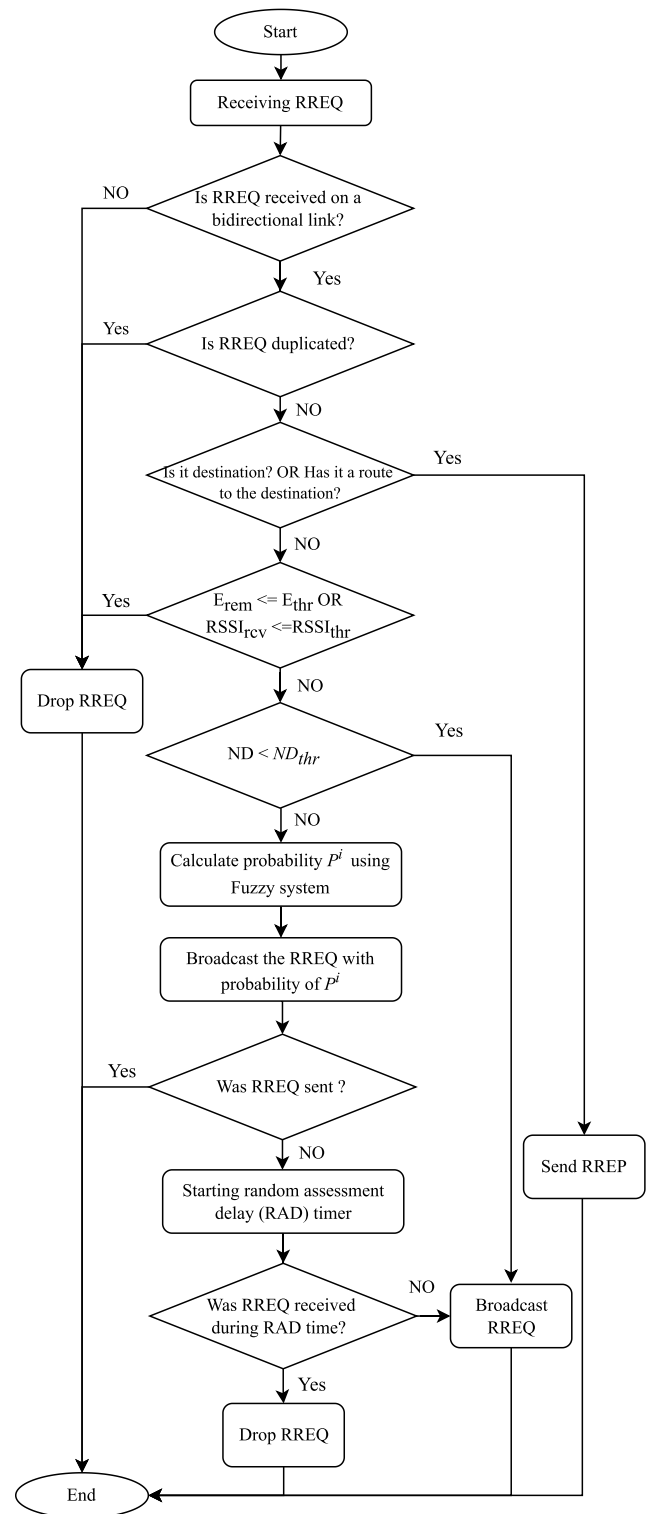


FIGURE 7. Proposed route discovery flowchart ($E_{thr} = \%1$, $RSSI_{thr} = 3.652622424e-10$, $ND_{thr} = 6$).

c: PATH QUALITY METRIC (PQM)

Path quality metric is a field in the modified RREQ message. This metric indicates the quality of the path on which the RREQ is received. If a mobile node receives an RREQ

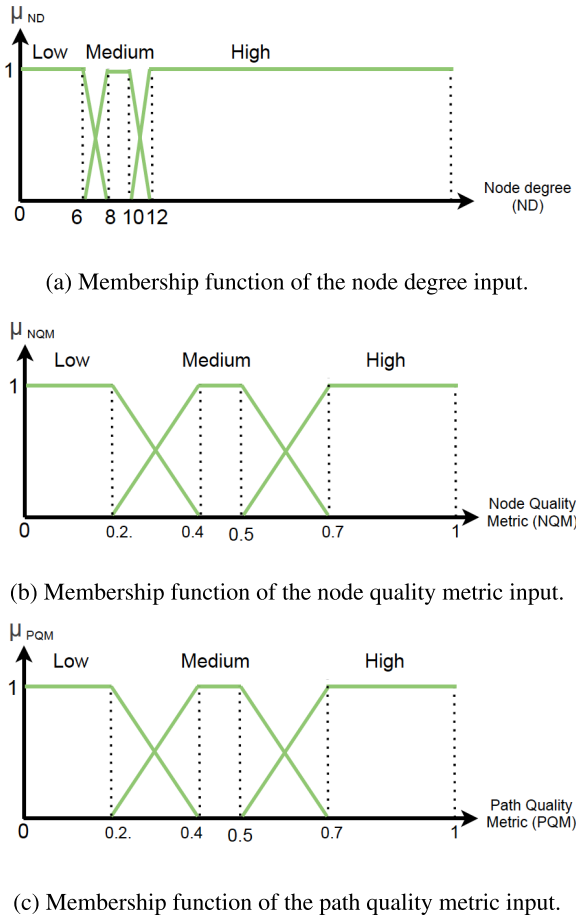


FIGURE 8. Fuzzy membership sets of the input variables for the broadcast decision-making module.

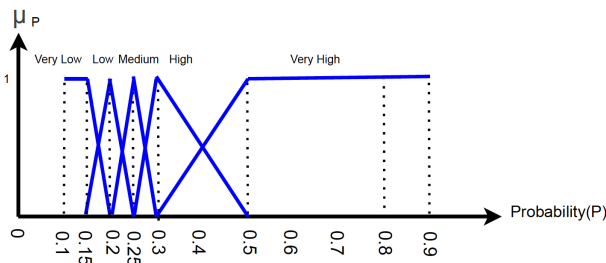


FIGURE 9. Fuzzy membership sets of the broadcast probability for the broadcast decision-making module.

message on a path with high quality, it rebroadcasts the message with a higher probability.

2) FUZZY OUTPUT

The defuzzified output value for the membership function at this stage is a number between 0.1 and 0.9 which is the probability P for broadcasting RREQ. To avoid the unreachability problem, we use the value 0.1 for the lower boundary of the probability. To defuzzify this, we again use the LOM. Since the mobile node broadcasts the RREQ packet with a

TABLE 4. Forwarding decision maker module rules. Input triples outline high (H), medium (M), and low (L) classifications for density, node quality, and path quality, respectively. Output labels include very low (VL), low (L), medium (M), high (H), and very high (VH).

Rule	Value	Output
1	(L, L, L)	M
2	(L, L, M)	M
3	(L, L, H)	H
4	(L, M, L)	M
5	(L, M, M)	M
6	(L, M, H)	VH
7	(L, H, L)	M
8	(L, H, M)	H
9	(L, H, H)	VH
10	(M, L, L)	L
11	(M, L, M)	M
12	(M, L, H)	M
13	(M, M, L)	L
14	(M, M, M)	M
15	(M, M, H)	H
16	(M, H, L)	M
17	(M, H, M)	M
18	(M, H, H)	H
19	(H, L, L)	VL
20	(H, L, M)	L
21	(H, L, H)	M
22	(H, M, L)	VL
23	(H, M, M)	L
24	(H, M, H)	M
25	(H, H, L)	VL
26	(H, H, M)	L
27	(H, H, H)	M

probability of P , it is possible that the packet is not sent at this stage. In this case, the algorithm enters Phase III to ensure that the packet is sent by a sufficient number of neighbours.

3) KNOWLEDGE BASE BLOCK

Three fuzzy sets with trapezoidal membership functions were defined for each of the input variables in the database. The three input linguistic variables were used to categorize the input parameters into three levels: low (L), medium (M), and high (H). Fig. 8 depicts the membership functions for input parameters. Three fuzzy sets are defined for three input parameters, leading to 27 rules for this module (Table 4).

The result of the broadcast decision-making module is the broadcast probability. This module suppresses the received broadcast with a probability of $1-P$. Five fuzzy sets (linguistic variables) with triangular membership functions have been used to describe the broadcast probability: very low, low, medium, high, and very high. Fig. 9 depicts the broadcast probability output membership function. The fuzzy inference engine for this module is based on Mamdani’s minimum. The Fuzzy Inference Engine (fuzzy decision-making unit) evaluates the fuzzy rules and produces an output for each rule based on the fuzzy input.

Phase III: If a node n failed to forward the RREQ to its neighbour at Phase II, it moves to a counter-based process in which it starts a random timer τ and waits to gather information about the environment to decide whether to rebroadcast or discard reject the received RREQ. Here, the node waits to receive a certain number of copies C of RREQ messages.

We use the random timer to reduce message contention and collision when nodes are near one another. If it has received C copies of the same RREQ from its neighbour, it means that the RREQ has been rebroadcasted as much as is necessary. Otherwise, it rebroadcasts the RREQ. By utilizing the counter-based phase we minimize the vulnerability to unreachability in our method.

To calculate random wait time, we use the AODV Node Traversal Time (NTT) parameter [5]. It estimates the typical one-hop traversal time for packets, including queuing delays, interrupt processing times, and transfer times. NTT is set to 30 ms (which can be accessed via “ns-2.35/aodv/aodv.h” in the NS 2.35 simulator). We calculate the random timer through the Eq. 11:

$$TMR_{rand} = \phi + NTT, \quad (11)$$

where TMR_{rand} is the random timer and ϕ is a random number between 0 to 60 ms.

This is repeated for each intermediate node until the RREQ reaches the destination. At that point, the destination node sends an RREP to the source node. These parameters are tuned by repeating the experiment.

C. ROUTE REPLY MECHANISM

Unlike the original version of AODV in which the destination node replies to the first received RREQ, in our proposed algorithm the quality of the paths and hop count are taken into account to provide an RREP message. As mentioned previously, RREQ is modified by adding the path quality metric (PQM) field to its original form as shown in Fig. 4. When an intermediate node receives an RREQ, it updates the value of the PQM value before rebroadcasting. This process is repeated until the destination node receives the RREQ. When the destination received the first RREQ, it starts a timer and stores all RREQs from the particular source before the timer ends. Next, the destination node calculates the path priority factor (PPF) as a function of PQM and hop count metric (HC) as shown in Eq. (12).

$$PPF = (\alpha \times PQM) (\beta \times HC)^{-1}, \quad (12)$$

where α and β are weights. The destination node then sends the RREP for the RREQ with the highest priority.

IV. SIMULATION SETTING

The proposed method is implemented using Network Simulator 2 (NS2.35). The parameters of the simulated network are listed in Table 5. Nodes are placed randomly in a 1000 m × 1000 m region. The transmission range for all nodes is 150 m. Nodes move around the area according to the random waypoint model which is one of the popular mobility models for the evaluation of routing protocols in MANETs. At the start, all nodes are randomly distributed in a given two-dimensional area and each node moves toward a random point at a random speed within the range $[V_{min}, V_{max}]$. When a node arrives at its destination, it waits for a pause time T_{pause} before repeating the process. Due to the limited transmission

TABLE 5. Parameter settings for the simulation study.

Parameter	Value
Routing protocol	AODV FP-AODV CLAF-AODV
MAC layer protocol	IEEE802.11b
TxPower, RxPower	2.7 dB
Transmission Range	150 m
Bandwidth	2 Mbps
Mobility model	Random Waypoint model
Pause time	2 s
Nodes Speed	1 m/s - 5 m/s
Number of nodes	100, 200, 300, 400, 500
Number of connections	10 (for scenario 1) 20 (for scenario 2)
Traffic Pattern	CBR,UDP
Message size	500 bytes
Simulation area	1000 m × 1000 m
Simulation Time	300 s

range, mobile nodes exchange packets in a multi-hop manner. The speed of the mobility is varied from 2 m/s to 5 m/s. To define variable network density, the number of nodes in the network ranges from 100 to 500. The simulation ran under various traffic loads with 10 and 20 Constant bitrate (CBR) connections for each number of nodes. Traffic is transmitted using User Datagram Protocol (UDP). To increase the accuracy of the estimate for the results, we repeat the experiment 30 times for each scenario. To reduce the impact of node distributions on simulation results, the random traffic connections are generated by using the same seed for different scenarios. The cbrgen.tcl script, a utility included in the NS-2.35 package that allows for the selection of traffic settings, was used to generate traffic. By using an Awk script to process data from trace files, we calculated the performance metrics.

V. SIMULATION RESULTS AND STATISTICAL ANALYSIS

We explore the performance of the CLAF-AODV routing protocol against both the AODV and FP-AODV routing protocols under varying conditions. To accomplish this goal, we developed several linear models using the lm function in R (version 4.0.4 [45]) to explore how our simulation parameters (e.g. the number of nodes (N_{nodes}), the routing protocol used, and the number of connections) affect the five performance metrics (i.e. normalized routing load, average end-to-end delay, packet loss, collision rate, and average energy consumption). To account for the possibility that the performance metrics might depend on the interaction of the simulation parameters, several two-way interaction terms were included in the model. The general structure of each model is described via:

$$\begin{aligned}
 y = & \beta_0 + \beta_1 \cdot N_{nodes} \\
 & + \beta_2 \cdot \mathbb{I}_{RP_{CLAF}} + \beta_3 \cdot \mathbb{I}_{RP_{FP}} + \beta_4 \cdot \mathbb{I}_{S_2} \\
 & + \beta_5 \cdot N_{nodes} \cdot \mathbb{I}_{RP_{CLAF}} + \beta_6 \cdot N_{nodes} \cdot \mathbb{I}_{RP_{FP}} \\
 & + \beta_7 \cdot N_{nodes} \cdot \mathbb{I}_{S_2} + \epsilon,
 \end{aligned}$$

where β_0 represents the baseline (i.e. AODV protocol and scenario 1) model intercept, β_1 represents the slope associated with the number of nodes in the experiment, $\beta_i, i = 2 \dots 4$ represent the change in intercept from baseline for the various factor variables, and $\beta_i, i = 5 \dots 7$ represent the change in slope from baseline for the number of nodes in the experiment given the factor variables. Factor variables are included via the indicator function \mathbb{I}_* , where \mathbb{I}_* is set to 1 if $*$ is true, and 0 otherwise. For example, $\mathbb{I}_{RP_{CLAF}} = 1$ if the CLAF-AODV routing protocol is used, and set to 0 otherwise. In this case, β_2 represents the average intercept difference between the CLAF-AODV protocol and the baseline method (i.e. the AODV protocol), and β_5 represents the average slope difference for the CLAF-AODV protocol compared to the baseline protocol. Similarly, β_3 and β_6 represent the average intercept and slope difference, respectively, for the case where $\mathbb{I}_{RP_{FP}} = 1$ compared to the AODV baseline. Further, $\mathbb{I}_{S_2} = 1$ in the case of scenario 2. Given this, β_4 and β_7 represent, respectively, the average intercept and slope difference compared to the scenario 1 baseline. Finally, ϵ represents a normal random error with mean 0, and variance σ^2 .

To show the effectiveness of the proposed protocol, we evaluate normalized routing load (NRL), average end-to-end delay (EED), packet loss, collision rate, and average energy consumption as performance metrics across the different scenarios and given the routing protocol and the number of nodes in each experiment. Simple contrasts are used to evaluate the statistical significance of the findings. We discuss the results for each performance metric in the following paragraphs.

A. NORMALIZED ROUTING LOAD (NRL)

The normalized routing load is calculated by dividing the total number of routing control packets (RREQ, RREP, RERR, etc.) transmitted by all nodes by the total number of data packets received at the destination nodes [46].

$$NRL = \frac{\sum RPK_{tx}}{\sum DPK_{rx}}, \quad (13)$$

where RPk_{tx} represents the sent routing packets and DPk_{rx} represents the received data packets.

Figure 10 compares the observed averages for NRL across the three protocols and 2 scenarios, given the number of nodes used in each experiment. Contrast results are shown in Table 6 for scenario 1. Similar results were found for scenario 2 but are not shown. As outlined in the table (and visible in the graph), there are no significant differences (i.e. $p\text{-value} > 0.05$) between the three routing protocols and across the two scenarios in the case of a MANET consisting of 100 nodes. However, for the case of 200 nodes and above, CLAF-AODV has a statistically significant difference in the routing load compared to both AODV and FP-AODV. For example, the average percent reduction in normalized routing load for CLAF-AODV compared to AODV and given scenario 2 were 54.9%, 66.5%, 72.6%, and 67.2% for 200, 300, 400, and 500 nodes, respectively. Scenario 1 saw a percent reduction ranging from 31.2% to 53.6%. CLAF-AODV also

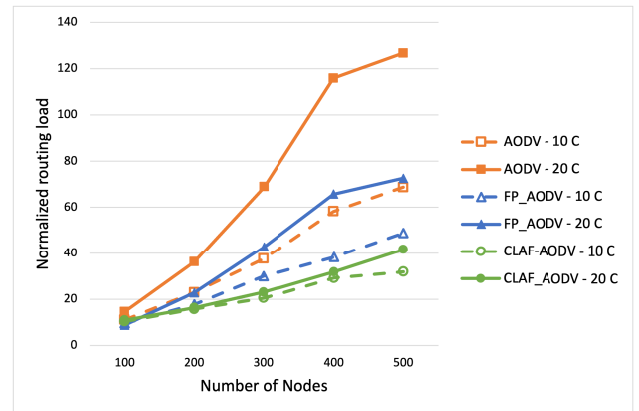


FIGURE 10. Normalized routing load vs number of nodes given three protocols (AODV [orange lines with boxes], FP-AODV [blue lines with triangles], and CLAF-AODV [green lines with circles]) and 2 scenarios (10 connections [dashed lines and hollow shapes] and 20 connections [solid lines and solid shapes]).

TABLE 6. Contrast estimates of normalized routing load for 100, 200, 300, 400, and 500 nodes. Significant differences ($p\text{-value} < 0.05$) are presented using boldfaced text. Negative values indicate that the first protocol listed in a row has a lower average normalized routing load than the second protocol listed in the same row.

	Normalized routing load				
Number of Nodes	100	200	300	400	500
CLAF vs AODV	-0.80	-16.87	-32.94	-49.01	-65.07
FP vs AODV	-1.89	-11.14	-20.38	-29.63	-38.88
CLAF vs FP	1.09	-5.73	-12.55	-19.37	-26.20

outperformed FP-AODV, with average percent reductions ranging from 11.1% to 34.6% (scenario 1) and 28.3% to 51.6% (scenario 2).

B. THROUGHPUT

The number of bits that are successfully received by the destination nodes in a period of time (t_{sim}) is known as throughput. Higher values of throughput reflect better network performance. Throughput, measured in kilobits per second (Kbps), is calculated by Eq. (14):

$$Throughput = (Byte_{rx} * 8) / (t_{sim} * 1024), \quad (14)$$

where $Byte_{rx}$ is the number of received bytes and t_{sim} is the simulation time.

The average throughput across experiments for each of the three protocols and 10 or 20 network connections is shown in Fig. 11. Contrast results for throughput are summarized in Table 7 for scenario 1. Again, similar results were found for scenario 2, but are not shown. Significant statistical differences in average throughput were identified in all comparisons save for the throughput comparison between FP-AODV and AODV and given 100 or 200 nodes in the network. Regardless, CLAF-AODV significantly outperformed both AODV and FP-AODV for both scenarios and given 100, 200, 300, 400, or 500 nodes. Specifically, CLAF-AODV saw significant increases in throughput ranging from 1.7% to 20.9% (scenario 1) and 5.9% to 36.7% (scenario 2) compared

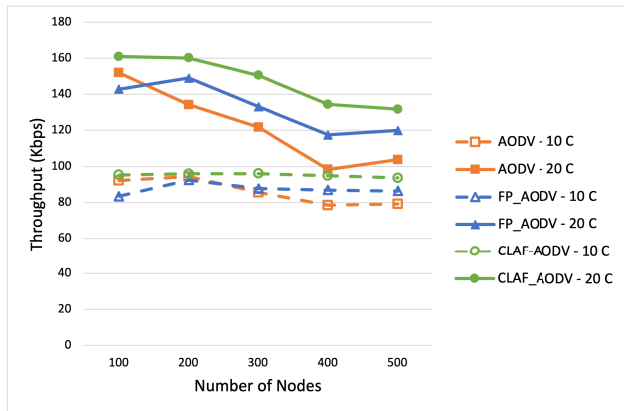


FIGURE 11. Throughput vs number of nodes given three protocols (AODV [orange lines with boxes], FP-AODV [blue lines with triangles], and CLAF-AODV [green lines with circles]) and 2 scenarios (10 connections [dashed lines and hollow shapes] and 20 connections [solid lines and solid shapes]).

TABLE 7. Contrast estimates of throughput for 100, 200, 300, 400, and 500 nodes. Significant differences (p-value < 0.05) are presented using boldfaced text. Positive values indicate that the first protocol listed in a row has a higher average throughput than the second protocol listed in the same row.

Number of Nodes	Throughput (Kbps)				
	100	200	300	400	500
CLAF vs AODV	8.80	13.09	17.39	21.68	25.98
FP vs AODV	-3.79	1.094	5.98	10.86	15.74
CLAF vs FP	12.59	12.00	11.41	10.83	10.24

to AODV, and 3.8% to 14.2% (scenario 1) and 7.5% to 14.5% (scenario 2) compared to FP-AODV.

C. AVERAGE END-TO-END DELAY (EED)

The average time taken by data packets to successfully transfer from a source to a destination node is referred to as end-to-end delay [47], and is calculated using the Eq. 15:

$$Average\ EED = \frac{1}{N} \sum (t_{rx} - t_{tx}), \quad (15)$$

where t_{rx} is the packet's received time, t_{tx} is the packet's sent time, and N is the total number of packets. The end-to-end delay performance comparison between AODV, FP-AODV, and CLAF-AODV are illustrated in Fig. 12. Again, CLAF-AODV outperforms both AODV and FP-AODV. Specifically, CLAF-AODV is shown to significantly reduce the average EED for both scenario 1 and 2, and given all network sizes considered. The minimum and maximum reductions observed in EED were 1.4% (scenario 1, CLAF-AODV vs AODV, 100 nodes), and 63.37% (scenario 1, CLAF-AODV vs AODV, 400 nodes), respectively.

Packet loss: Packet loss is defined as the percentage of transmitted packets that were not received by the destination nodes [48].

$$Packet\ loss = \left(\sum P_{tx} - \sum P_{rx} \right) / \sum P_{tx} \quad (16)$$

where P_{tx} is the sent packet and P_{rx} is received packet.

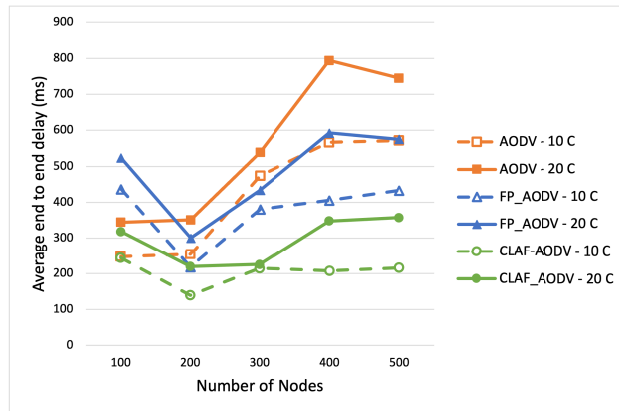


FIGURE 12. Average end-to-end delay vs number of nodes given three protocols (AODV [orange lines with boxes], FP-AODV [blue lines with triangles], and CLAF-AODV [green lines with circles]) and 2 scenarios (10 connections [dashed lines and hollow shapes] and 20 connections [solid lines and solid shapes]).

TABLE 8. Contrast estimates of Average end-to-end delay for 100, 200, 300, 400, and 500 nodes. Significant differences (p-value < 0.05) are presented using boldfaced text. Negative values indicate that the first protocol listed in a row has a lower average end-to-end delay than the second protocol listed in the same row.

Number of Nodes	Average end-to-end delay ($\times 10^2$)				
	100	200	300	400	500
CLAF vs AODV	-0.41	-1.41	-2.40	-3.39	-4.39
FP vs AODV	1.04	0.23	-0.59	-1.40	-2.22
CLAF vs FP	-1.45	-1.63	-1.81	-1.99	-2.17

TABLE 9. Contrast estimates of packet loss for 100, 200, 300, 400, and 500 nodes. Significant differences (p-value < 0.05) are presented using boldfaced text. Negative values indicate that the first protocol listed in a row has a lower average packet loss than the second protocol listed in the same row.

Number of Nodes	Packet loss				
	100	200	300	400	500
CLAF vs AODV	-3.25	-7.80	-12.34	-16.89	-21.43
FP vs AODV	3.77	0.203	-3.36	-6.93	-10.50
CLAF vs FP	-7.03	-8.00	-8.98	-9.95	-10.93

where P_{tx} are sent packets and P_{rx} are received packets. Excessive redundant broadcast packets lead to packet loss by exhausting the network resources. Fig. 13 depicts the results for packet loss. Contrast estimates (Table 9) indicate that CLAF-AODV significantly outperforms both AODV and FP-AODV given both scenarios and all network sizes. The range in packet loss is 6.1% to 62.9% (scenario 1, CLAF-AODV vs AODV), 40.1% to 47.7% (scenario 1, CLAF-AODV vs FP-AODV), 12.0% to 57.6% (scenario 2, CLAF-AODV vs AODV), and 26.4% to 45.5% (scenario 2, CLAF-AODV vs FP-AODV).

D. MAC COLLISION RATE

represents the average number of packets discarded per second as a result of MAC layer collisions. Mac collision rate is

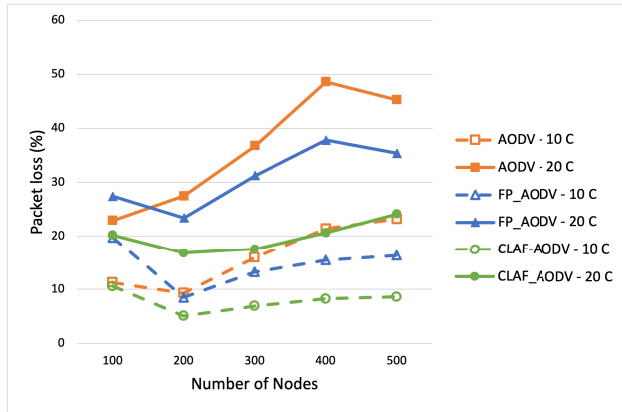


FIGURE 13. Packet loss vs number of nodes given three protocols (AODV [orange lines with boxes], FP-AODV [blue lines with triangles], and CLAF-AODV [green lines with circles]) and 2 scenarios (10 connections [dashed lines and hollow shapes] and 20 connections [solid lines and solid shapes]).

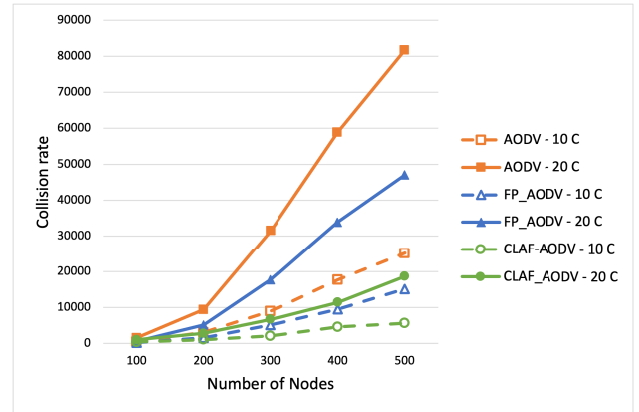


FIGURE 14. Collision rate vs number of nodes given three protocols (AODV [orange lines with boxes], FP-AODV [blue lines with triangles], and CLAF-AODV [green lines with circles]) and 2 scenarios (10 connections [dashed lines and hollow shapes] and 20 connections [solid lines and solid shapes]).

calculated using Eq. (17):

$$MAC\ collision\ rate = \frac{1}{t_{sim}} \sum P_{drop}, \quad (17)$$

where P_{drop} is the dropped packet at the MAC layer and t_{sim} is the simulation time. As previously discussed, the number of duplicate broadcast packets rose as node density increased. With more duplicate broadcast packets, channel contention increased. Mobile nodes in MANETs operate on shared wireless channels. Medium contention at the MAC layer is a mechanism used by mobile nodes to ensure that shared wireless media are used efficiently (Section III-A for more detail). Channel contention increases by increasing the number of traffic that attempts to access the shared wireless channel. Increasing contention results in increasing EED because of the high probability of several back-off for transmitting a packet. In addition, due to a limited number of re-transmissions (for TCP (Transmission Control Protocol) traffic), increasing contention can lead to packet loss and decreased throughput.

Fig. 14 displays the rate of collisions across both scenarios, the five network sizes, and for each of the protocols evaluated. Table 10 provides a summary of the contrast estimates. CLAF-AODV results were significantly lower than the other protocols considered for both scenarios and given the network size, except for the comparison between CLAF-AODV and FP-AODV given 100 nodes. In this case, no significant difference was observed. Regardless, the statistically significant reductions ranged from 17.3% to 77.7% (scenario 1, CLAF-AODV vs AODV), 30.7% to 62.9% (scenario 1, CLAF-AODV vs FP-AODV), 35.6% to 80.6% (scenario 2, CLAF-AODV vs AODV), and 44.9% to 66.3% (scenario 2, CLAF-AODV vs FP-AODV).

E. AVERAGE ENERGY CONSUMPTION

represents the average energy consumed by the network nodes during the simulation. It is calculated via

TABLE 10. Contrast estimates of MAC collision rate for 100, 200, 300, 400, and 500 nodes. Significant differences (p-value < 0.05) are presented using boldfaced text. Negative values indicate that the first protocol listed in a row has a lower average MAC collision rate than the second protocol listed in the same row.

Number of Nodes	MAC Collision rate ($\times 10^2$)				
	100	200	300	400	500
CLAF vs AODV	31.74	-76.17	-184.07	-291.98	-399.94
FP vs AODV	11.86	-45.36	-102.59	-159.82	-217.12
CLAF vs FP	19.88	-30.80	-184.07	-132.16	-182.84

Eq. (18):

$$E_{avg} = \frac{1}{n} \sum_{i=1}^n (E_{ini}^i - E_{rem}^i), \quad (18)$$

where E_{ini}^i is the initial energy of node i , E_{rem}^i is the remaining energy of node i at the end of simulation time, and n is the number of network nodes.

Mobile nodes consume energy to transmit packets. Reducing the number of transmitted packets reduces energy consumption. Fig. 15 portrays the energy consumption for each of the 3 protocols evaluated, for 2 scenarios, and given different network sizes. CLAF-AODV showed significant reductions in energy consumption compared to the AODV and FP-AODV protocols, except for three scenario 1 cases: there was no significant difference between 1) CLAF-AODV and AODV given 100 nodes, nor 2) between CLAF and FP given 200 nodes. In case 3, we observed a significant increase in energy consumption between CLAF-AODV and FP-AODV for 100 nodes. These patterns were consistent for scenario 2 as well. Contrast estimates can be found in Table 11.

VI. DISCUSSION

Although Broadcasting as a common mechanism of MANET routing algorithms increases the reachability of the network, however, it can result in broadcast storm problems in high-density environments. Broadcast storms occur when a huge

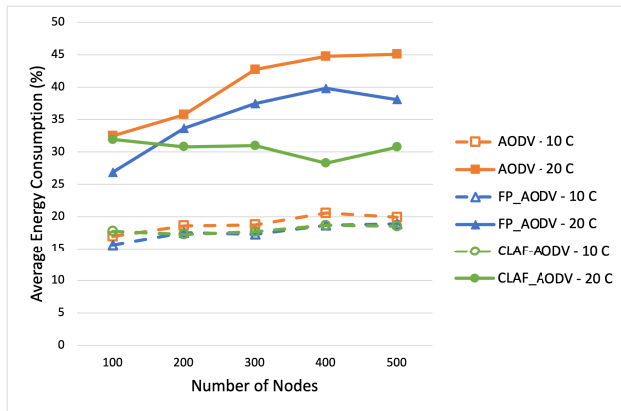


FIGURE 15. Average energy consumption vs number of nodes given three protocols (AODV [orange lines with boxes], FP-AODV [blue lines with triangles], and CLAF-AODV [green lines with circles]) and 2 scenarios (10 connections [dashed lines and hollow shapes] and 20 connections [solid lines and solid shapes]).

TABLE 11. Contrast estimates of average energy consumption for 100, 200, 300, 400, and 500 nodes. Significant differences (p -value < 0.05) are presented using boldfaced text. Negative values indicate that the first protocol listed in a row has a lower average energy consumption than the second protocol listed in the same row.

Number of Nodes	Average energy consumption				
	100	200	300	400	500
CLAF vs AODV	-0.44	-1.55	-2.65	-3.75	-4.85
FP vs AODV	-1.29	-1.44	-1.59	-1.73	-1.88
CLAF vs FP	0.85	-0.10	-1.06	-2.01	-2.96

number of broadcast packets are in the network in a short period of time. When the number of nodes increases in a specific area, the number of broadcast packets increases exponentially. These redundant packets waste network resources and impair network performance.

Although many protocols have been proposed to solve the stated problem, as far as we know, none have considered sufficient parameters simultaneously in their proposed algorithm to reduce the number of broadcasts and increase QoS. Nodes in our proposed protocol decide whether to broadcast packets based on several factors from different layers of the OSI model which can affect network adaptability, stability, and service quality (Sections III-A1 and III-B). In the rest of this section we discuss the results of our simulation study.

A. NORMALIZED ROUTING LOAD

Excess routing packets (i.e. overhead) are undesired traffic that consumes network resources and increases contention, ultimately reducing network performance. As such, improving network performance requires lowering routing overhead. In this paper, we showed that the normalized routing load observed for AODV, FP-AODV, and the proposed CLAF-AODV were not statistically significantly different when the network was small (100 nodes). This is likely due to the sparse nature of the network (i.e. 100 mobile nodes in $1000 m^2$ with a transmission range of $150m$)

where it is expected that nodes won't always receive every broadcast packet. Regardless, as the network size increased, CLAF-AODV significantly outperformed both AODV and FP-AODV (Fig. 10). Further, the normalized routing load increased more than 6.2 (scenario 1) to 8.7 (scenario 2) for the AODV protocol, and by more than 5.1 (scenario 1) to 8.3 (scenario 2) times for the FP-AODV protocol (as the network size grew from 100 to 500 nodes). This compared to an increase of only 3.1 and 3.8 times for the proposed CLAF-AODV protocol given scenarios 1 and 2, respectively. These findings suggest that the fuzzy logic decision making algorithms used in the proposed protocol improves network performance since it considers the quality of each node and path before retransmitting a packet; something that neither AODV or FP-AODV do. Further, the use of a fixed probability (in our case, $P = 0.65$) in the FP-AODV protocol may not be sufficient to account for the heterogeneity of the network, nor the manner in which the local density varies across the network. CLAF-AODV considers heterogeneous node density to calculate rebroadcast probabilities from 10% for a high-density environment to 90% for a low-density environment using a fuzzy logic system if the number of neighbouring nodes is 6 or higher. Otherwise, CLAF-AODV operates the same as AODV. Finally, to avoid early death, CLAF-AODV follows a counter-based approach (Section III-B). All of these considerations work together to provide an appropriate dynamic broadcasting decision in CLAF-AODV to reduce redundant routing packets.

B. THROUGHOUT

The rate of successfully delivered messages through the network in a given amount of time is referred to as network throughput, and is a key indicator of performance. Some parameters in the network (e.g. bandwidth, network congestion, end-to-end delay, and packet loss) can affect network throughput. Our simulation study demonstrates that the CLAF-AODV protocol allows for significantly higher throughput compared to the AODV and FP-AODV protocols for all network sizes and for both scenario 1 or 2 (Fig. 11). Further, CLAF-AODV throughput was relatively unchanged for scenario 1 (decreasing by less than 2%), and decreased by approximately 20% for scenario 2 (when the number of nodes increased from 100 to 500). The AODV protocol saw reductions of roughly 15% and 32% across the two scenarios, compared to an increase of about 4% and a reduction of 16% for FP-AODV. In other words, CLAF-AODV provided higher levels of throughput and smaller reductions in throughput as the network size increased (for either scenario) compared to both the AODV and FP-AODV protocols.

C. AVERAGE END-TO-END DELAY (EED)

More redundant broadcast packets are generated in higher node density which causes a higher probability of network congestion and collision. Collisions can result in excessive retransmission and lead to channel contention - both of which increase EED. In high-density MANETs, the

AODV and FP-AODV protocols do not perform as well as the CLAF-AODV protocol in terms of end-to-end delay. In fact, the CLAF-AODV protocol significantly outperforms the other two protocols investigated. Comparing the change in end-to-end delay as the network size increased from 100 to 500 nodes, the AODV protocol saw end-to-end delay increased by 131% (scenario 1) and 117% (scenario 2). The FP-AODV protocol, however, provided a reduction of less than 1% in end-to-end delay for scenario 1, and an increase of roughly 10% for scenario 2. This compares to the CLAF-AODV protocol which reported a reduction of approximately 11% for scenario 1, and an increase of approximately 12% for scenario 2. That is, we have a case where CLAF-AODV typically has lower end-to-end delay than the other two protocols, and the changes in end-to-end delay as the network size increases is typically smaller than the change observed for AODV and FP-AODV. This is likely due to the fact that in the CLAF-AODV protocol, the chance of choosing nodes to participate in routing is determined by the levels of contention, the length of the queue, and the amount of available bandwidth - all of which directly affect end-to-end delay.

D. PACKET LOSS

Packet loss occurs when one or more packets on a computer network are unable to reach their destination. It is a more serious problem for wireless networks than wired networks, where loss can occur due to network congestion, radio frequency interference, degraded signals, distance, physical obstacles, and limitations in network bandwidth, buffer capacity, or other constrained network resources. As such, routing protocols should be designed to reduce packet loss as much as possible. Reducing redundant broadcast packets and efficiently using network resources are two ways to reduce congestion and packet loss. Since the CLAF-AODV protocol was designed to do exactly this, it is not surprising that the protocol significantly outperformed both the AODV and FP-AODV approaches. That is, CLAF-AODV had significantly fewer lost packets compared to the other protocols. Further, as the network size increased from 100 to 500 nodes, the CLAF-AODV protocol saw a decrease of approximately 18% in the number of packets lost given scenario 1, and an increase of about 19% given scenario 2. This compares to an increase of 106% and 98% packet loss for AODV given the two scenarios, a decrease of approximately 17% (scenario 1), and an increase of approximately 29% (scenario 2) for FP-AODV. In other words, the relative changes in packet loss as the network size grows from 100 to 500 nodes for FP-AODV and CLAF-AODV are relatively similar (although FP-AODV has a larger increase for scenario 2), but the CLAF-AODV protocol typically starts with a lower values of packet loss. Further work should investigate if these patterns hold for larger network sizes, as there may be a point at which FP-AODV outperforms CLAF-AODV.

E. MAC COLLISION RATE

Mobile devices communicate on wireless shared channels. A network collision occurs when two or more devices try to access the same shared channel at the same time. The collision of radio signals causes data loss and corruption. To prevent collision in the wireless channel, wireless devices employ a form of contention to avoid collision. Backoff is a common strategy that is used by wireless devices to resolve contention problems (Section III-A1). Increasing network traffic can lead to increases in backoff to transmit packets and result in high end-to-end delay or even packet drop. Additionally, restrictions on retransmission of a transmitted packet may result in packet loss. The CLAF-AODV protocol was found to significantly reduce network collision and contention (compared to the AODV and FP-AODV protocols for both scenarios and network sizes above 100 nodes) by reducing redundant rebroadcasts. Selecting potential mobile nodes to form routing paths by considering the channel status in terms of collisions appears to provide better network performance in terms of end-to-end delay and packet loss. In the case of 100 nodes, the CLAF-AODV collision rate was not significantly different from FP-AODV, but was significantly higher than AODV. As the network size increased, the CLAF-AODV collision rate increased by a factor of approximately 14 for scenario 1, and by a factor of approximately 18 for scenario 2. This compares to increases by a factor of 51 for AODV (both scenarios), and increases by a factor of 61 and 75 for FP-AODV (scenario 1 and scenario 2, respectively). Again, the proposed CLAF-AODV algorithm tends to have significantly lower collision rates (for larger networks), and the change in collision rate as the network grows tends to be smaller compared to the other two protocols.

F. AVERAGE ENERGY CONSUMPTION

Mobile devices rely on the limited power supplied by their battery. Network lifetime is therefore improved by decreasing energy consumption. Since mobile nodes consume energy to transmit and receive packets (based on our energy model), reducing overhead can lead to fewer rebroadcast packets and an overall reduction in energy consumption compared to the competing protocols. Given the design of the CLAF-AODV protocol, we find that energy consumption for larger networks is typically significantly reduced compared to the AODV and FP-AODV protocols. This is not necessarily the case for smaller networks, where the energy consumption is found not statistically significantly different at 100 nodes (CLAF-AODV vs. AODV), and 200 nodes (CLAF-AODV vs. FP-AODV), and is in fact significantly greater at 100 nodes when comparing CLAF-AODV to FP-AODV. The change in energy consumption is also important to consider. In the case of the CLAF-AODV protocol, energy consumption increases by approximately 4% for scenario 1, and decreases by approximately 4% for scenario 2 as the network grows from 100 to 500 nodes. In contrast, the FP-AODV protocol increases by 20% and 42%, and the AODV protocol increases

by 17% and 39% for scenarios 1 and 2, respectively. In other words, the CLAF-AODV typically outperforms the other protocols, and sees smaller increases in energy consumption as the network grows.

VII. CONCLUSION

In this work, we proposed the novel CLAF-AODV routing protocol to cope with the broadcast problem. We leveraged two-level fuzzy logic to suppress broadcast packets in the network. The proposed protocol considered stability, quality, and adaptability factors to make the appropriate decision about forwarding broadcast packets. For this purpose, the forwarding probability is calculated adaptively based on parameters such as node quality, path quality, and network density around a node. We employed fuzzy logic to determine node quality based on energy, bandwidth, the length of the queue, signal strength, and MAC contention as inputs. Our simulation study and analysis demonstrate that compared to the original AODV and FP-AODV protocols, our proposed routing protocol decreases routing load and MAC layer contention efficiently. The CLAF-AODV shows higher performance in terms of throughput, packet loss, and end-to-end delay in contrast to the two other routing protocols in a high network density. We will assess the suggested protocol using various node speeds and mobility models in our upcoming study. Then, to suggest an adaptive broadcasting strategy, we will take into account the mobility pattern and relative node speed in addition to the aforementioned characteristics. Further, routing protocols should be tested in *the field* since simulation studies do not necessarily capture environmental factors that might impact the functionality of a MANET.

ACKNOWLEDGMENT

The Dish With One Spoon Covenant speaks to their collective responsibility to steward and sustain the land and environment in which they live and work, so that all peoples, present and future, may benefit from the sustenance it provides. As they continue to strive to strengthen their relationships with and continue to learn from their Indigenous neighbors, they recognize the partnerships and knowledge that have guided the learning and research conducted as part of this work. They acknowledge that the University of Guelph resides in the ancestral and treaty lands of several Indigenous peoples, including the Attawandaron people and the Mississaugas of the Credit, and they recognize and honor their Anishinaabeg, Haudenosaunee, and M-tis neighbors. They also acknowledge that the work presented here occurred on their traditional lands so that they might work to build lasting partnerships that respect, honor, and value the culture, traditions, and wisdom of those who have lived here since time immemorial.

REFERENCES

- [1] D. Ramphull, A. Mungur, S. Armoogum, and S. Pudaruth, "A review of mobile ad hoc network (MANET) protocols and their applications," in *Proc. 5th Int. Conf. Intell. Comput. Control Syst. (ICICCS)*, May 2021, pp. 204–211.
- [2] F. Safari, I. Savić, H. Kunze, and D. Gillis, "The diverse technology of MANETs: A survey of applications and challenges," *Int. J. Future Comput. Commun.*, vol. 12, no. 2, 2023.
- [3] D. E. M. Ahmed and O. O. Khalifa, "An overview of MANETs: Applications, characteristics, challenges and recent issues," *Int. J. Eng. Adv. Technol.*, vol. 6, no. 4, pp. 128–133, 2017.
- [4] T. K. Saini and S. C. Sharma, "Prominent unicast routing protocols for mobile ad hoc networks: Criterion, classification, and key attributes," *Ad Hoc Netw.*, vol. 89, pp. 58–77, Jun. 2019.
- [5] Z. J. Haas, J. Y. Halpern, and L. Li, "Gossip-based ad hoc routing," in *Proc. 21st Annu. Joint Conf. IEEE Comput. Commun. Soc.*, vol. 3, Jun. 2002, pp. 1707–1716.
- [6] B. H. Khudayer, M. Anbar, S. M. Hanshi, and T. Wan, "Efficient route discovery and link failure detection mechanisms for source routing protocol in mobile ad-hoc networks," *IEEE Access*, vol. 8, pp. 24019–24032, 2020.
- [7] M. A. Gawas, L. J. Gudino, and K. R. Anupama, "Cross layered adaptive cooperative routing mode in mobile ad hoc networks," in *Proc. 22nd Asia-Pacific Conf. Commun. (APCC)*, Aug. 2016, pp. 462–469.
- [8] Q. Zhang and D. P. Agrawal, "Dynamic probabilistic broadcasting in MANETs," *J. Parallel Distrib. Comput.*, vol. 65, no. 2, pp. 220–233, Feb. 2005.
- [9] P. Ruiz and P. Bouvry, "Survey on broadcast algorithms for mobile ad hoc networks," *ACM Comput. Surv.*, vol. 48, no. 1, pp. 1–35, Sep. 2015.
- [10] S. R. Das, C. E. Perkins, and E. M. Belding-Royer, *Ad Hoc On-Demand Distance Vector (AODV) Routing*, document RFC 3561, RFC Editor, Jul. 2003. [Online]. Available: <https://www.rfc-editor.org/info/rfc3561>, doi: 10.17487/RFC3561.
- [11] Y.-C. Tseng, S.-Y. Ni, Y.-S. Chen, and J.-P. Sheu, "The broadcast storm problem in a mobile ad hoc network," *Wireless Netw.*, vol. 8, nos. 2–3, pp. 153–167, 2002.
- [12] I. Stojmenovic and J. Wu, "Broadcasting and activity scheduling in ad hoc networks," *Mobile Ad Hoc Netw.*, pp. 205–229, Jun. 2004.
- [13] V. R. Kavitha and M. Moorthi, "A quality of service load balanced connected dominating set–stochastic diffusion search (CDS–SDS) network backbone for MANET," *Comput. Netw.*, vol. 151, pp. 124–131, Mar. 2019.
- [14] L. Zhang, L. Hu, F. Hu, Z. Ye, X. Li, and S. Kumar, "Enhanced OLSR routing for airborne networks with multi-beam directional antennas," *Ad Hoc Netw.*, vol. 102, May 2020, Art. no. 102116.
- [15] X. Huang, Y. Qing, and Y. Bao, "A distributed algorithm for virtual backbone construction in wireless networks," in *Proc. Int. Conf. Commun. Signal Process. (ICCS)*, Apr. 2018, pp. 0045–0049.
- [16] R. C. Gómez, I. Gonzalez-Herrera, Y. Bromberg, L. Réveillère, and E. Rivière, "Density and mobility-driven evaluation of broadcast algorithms for MANETs," in *Proc. IEEE 37th Int. Conf. Distrib. Comput. Syst. (ICDCS)*, Jun. 2017, pp. 2308–2313.
- [17] Y.-C. Tseng, S.-Y. Ni, and E.-Y. Shih, "Adaptive approaches to relieving broadcast storms in a wireless multihop mobile ad hoc network," *IEEE Trans. Comput.*, vol. 52, no. 5, pp. 545–557, May 2003.
- [18] M. B. Yassein, S. F. Nimer, and A. Y. Al-Dubai, "A new dynamic counter-based broadcasting scheme for mobile ad hoc networks," *Simul. Model. Pract. Theory*, vol. 19, no. 1, pp. 553–563, Jan. 2011.
- [19] S. O. Al-Humoud, L. M. Mackenzie, and J. Abdulai, "Neighbourhood-aware counter-based broadcast scheme for wireless ad hoc networks," in *Proc. IEEE Globecom Workshops*, Nov. 2008, pp. 1–6.
- [20] D. G. Reina, S. L. Toral, P. Johnson, and F. Barrero, "A survey on probabilistic broadcast schemes for wireless ad hoc networks," *Ad Hoc Netw.*, vol. 25, pp. 263–292, Feb. 2015.
- [21] S.-Y. Ni, Y.-C. Tseng, Y.-S. Chen, and J.-P. Sheu, "The broadcast storm problem in a mobile ad hoc network," in *Proc. 5th Annu. ACM/IEEE Int. Conf. Mobile Comput. Netw.*, Aug. 1999, pp. 151–162.
- [22] N. Nissar, N. Naja, and A. Jamali, "A review and a new approach to reduce routing overhead in MANETs," *Wireless Netw.*, vol. 21, no. 4, pp. 1119–1139, May 2015.
- [23] K. Mariyappan, "Gossip based node residual energy AODV routing protocol for ad-hoc network (GBNRE-AODV)," *Int. J. Adv. Res. Comput. Sci.*, vol. 8, no. 8, pp. 193–202, Aug. 2017.
- [24] A. Banerjee and S. Ghosh, "FPR: Fuzzy controlled probabilistic rebroadcast in mobile ad hoc network," *Int. J. Inf. Technol.*, vol. 12, no. 2, pp. 523–529, Jun. 2020.
- [25] S. Chettibi and S. Chikhi, "Dynamic fuzzy logic and reinforcement learning for adaptive energy efficient routing in mobile ad-hoc networks," *Appl. Soft Comput.*, vol. 38, pp. 321–328, Jan. 2016.

- [26] D. Driankov, H. Hellendoorn, and M. Reinfrank, *An Introduction to Fuzzy Control*. Springer, 2013.
- [27] W. K. Lai and C. Chiu, "Probabilistic second-chance broadcasting with/without global positioning system information in wireless ad hoc networks," *IEEE Access*, vol. 8, pp. 212608–212622, 2020.
- [28] X. Zhang, K. Chen, Y. Zhang, and D. K. Sung, "A probabilistic broadcast algorithm based on the connectivity information of predictable rendezvous nodes in mobile ad hoc networks," in *Proc. 23rd Int. Conf. Comput. Commun. Netw. (ICCCN)*, Aug. 2014, pp. 1–6.
- [29] F. J. Ovalle-Martínez, A. Nayak, I. Stojmenovic, J. Carle, and D. Simplot-Ryl, "Area-based beaconless reliable broadcasting in sensor networks," *Int. J. Sensor Netw.*, vol. 1, nos. 1–2, pp. 20–33, 2006.
- [30] K. Chandravanshi and D. K. Mishra, "Minimization of routing overhead on the bases of multipath and destination distance estimation mechanism under MANET," in *Proc. Int. Conf. ICT Bus. Ind. Government (ICTBIG)*, 2016, pp. 1–6.
- [31] F. Yu, E. Lee, S. Park, and S.-H. Kim, "A simple location propagation scheme for mobile sink in wireless sensor networks," *IEEE Commun. Lett.*, vol. 14, no. 4, pp. 321–323, Apr. 2010.
- [32] R. Rab, S. A. D. Sagar, N. Sakib, A. Haque, M. Islam, and A. Rahman, "Improved self-pruning for broadcasting in ad hoc wireless networks," *Wireless Sensor Netw.*, vol. 9, no. 2, pp. 73–86, 2017.
- [33] W. Peng and X.-C. Lu, "On the reduction of broadcast redundancy in mobile ad hoc networks," in *Proc. 1st Annu. Workshop Mobile Ad Hoc Netw. Comput. (MobiHOC)*, 2000, pp. 129–130.
- [34] T. T. Anannya and A. Rahman, "Extended neighborhood knowledge based dominant pruning (ExDP)," in *Proc. 5th Int. Conf. Netw., Syst. Secur. (NSysS)*, Dec. 2018, pp. 1–9.
- [35] B. Williams and T. Camp, "Comparison of broadcasting techniques for mobile ad hoc networks," in *Proc. 3rd ACM Int. Symp. Mobile Ad Hoc Netw. Comput.*, Jun. 2002, pp. 194–205.
- [36] A. Mohammed, M. Ould-Khaoua, and L. Mackenzie, "An efficient counter-based broadcast scheme for mobile ad hoc networks," in *Proc. Eur. Perform. Eng. Workshop*. Berlin, Germany: Springer, 2007, pp. 275–283.
- [37] A. M. E. Ejmaa, S. Subramaniam, Z. A. Zukarnain, and Z. M. Hanapi, "Neighbor-based dynamic connectivity factor routing protocol for mobile ad hoc network," *IEEE Access*, vol. 4, pp. 8053–8064, 2016.
- [38] Y. H. Robinson, R. S. Krishnan, E. G. Julie, R. Kumar, L. H. Son, and P. H. Thong, "Neighbor knowledge-based rebroadcast algorithm for minimizing the routing overhead in mobile ad-hoc networks," *Ad Hoc Netw.*, vol. 93, Oct. 2019, Art. no. 101896.
- [39] I. Savić, M. Asch, K. Rourke, F. Safari, P. Houlding, J. F. D. Veubeke, J. Ernst, and D. Gillis, "M-ODD: A standard protocol for reporting MANET related models, simulations, and findings," in *Proc. Ad Hoc Netw. Tools IT, 13th EAI Int. Conf. ADHOCNETS, 16th EAI Int. Conf. TRIDENTCOM*. Cham, Switzerland: Springer, 2022, pp. 114–129.
- [40] C. Perkins, E. Belding-Royer, and S. Das, *Ad Hoc On-Demand Distance Vector (AODV) Routing*, document RFC 3561, RFC Editor, Jul. 2003. [Online]. Available: <http://www.rfc-editor.org/rfc/rfc3561.txt>
- [41] L. A. Zadeh, "Fuzzy sets," in *Fuzzy Sets, Fuzzy Logic, and Fuzzy Systems: Selected Papers*. Singapore: World Scientific, 1996, pp. 394–432.
- [42] D. Ibrahim, "An overview of soft computing," *Proc. Comput. Sci.*, vol. 102, pp. 34–38, Jan. 2016.
- [43] M. M. Islam, M. A. Uddin, A. N. Bahar, A. K. Islam, and M. S. A. Mamun, "Energy efficient routing mechanism for mobile ad hoc networks," *Int. J. Comput. Sci. Eng.*, vol. 3, no. 1, pp. 9–20, 2014.
- [44] S. Zheng, L. Li, and Y. Li, "A QoS routing protocol for mobile ad hoc networks based on multipath," *J. Netw.*, vol. 7, no. 4, p. 691, Apr. 2012.
- [45] R Core Team, "R: A language and environment for statistical computing," R Found. Stat. Comput., Vienna, Austria, 2021. [Online]. Available: <https://www.R-project.org/>
- [46] F. Palmieri, "A wave propagation-based adaptive probabilistic broadcast containment strategy for reactive MANET routing protocols," *Pervas. Mobile Comput.*, vol. 40, pp. 628–638, Sep. 2017.
- [47] D. Bisen and S. Sharma, "An energy-efficient routing approach for performance enhancement of MANET through adaptive neuro-fuzzy inference system," *Int. J. Fuzzy Syst.*, vol. 20, no. 8, pp. 2693–2708, Dec. 2018.
- [48] K. L. Arega, G. Raga, and R. Bareto, "Survey on performance analysis of AODV, DSR and DSDV in MANET," *Comput. Eng. Intell. Syst.*, vol. 11, no. 3, pp. 23–32, 2020.



FATEMEH SAFARI received the B.Sc. degree in computer hardware engineering from Shiraz University, Shiraz, Iran, and the M.Sc. degree in IT engineering—computer networks from Amirkabir University, Tehran, Iran, with a focus on software-defined networking (SDN). She is currently pursuing the Ph.D. degree with the Computational Science Program, University of Guelph. She has several years of professional industry experience in the field of computer networks and routing protocols. She joins the Bridging the Digital Divide project to help people around the globe with better access and connectivity given limited network infrastructure.



HERB KUNZE received the Ph.D. degree in applied mathematics from the University of Waterloo, Waterloo, Canada, in 1997. He is currently a Professor of mathematics with the Department of Mathematics and Statistics, University of Guelph, Guelph, Canada. He has published more than 120 scientific articles and books in the broad area of applied analysis. His research interests include artificial intelligence, inverse problems, multi-criteria decision-making, and fractal-based methods in analysis.



JASON ERNST received the B.Sc. degree (Hons.) in computer science from Wilfrid Laurier University, Canada, and the M.Sc. and Ph.D. degrees in computer science in the area of wireless mesh networking from the University of Guelph, Canada. He co-founded a company called RightMesh which enabled mobile phones to form opportunistic mesh networks using Bluetooth, Wi-Fi, and Wi-Fi Direct. He is currently a Principal Software Engineer at a Boston-based mesh network startup.



DANIEL GILLIS is currently an Associate Professor and a Statistician with the School of Computer Science, University of Guelph. He spends most of his time working on interdisciplinary teams which have focused on public health assessment, natural resource management, software design, and pedagogy. Most recently, he has been with the Inuit of Rigolet, Nunatsiavut, and Labrador to develop mobile applications for environment and health monitoring and to develop tools to address a lack of internet and cellular infrastructure in the Circumpolar North.

...